Supplement of

Influence of mineral dust and sea spray supermicron particle concentrations and acidity on inorganic NO_3^- aerosol during the 2013 Southern Oxidant and Aerosol Study

H. M. Allen et al.

Correspondence to: J. L. Fry (fry@reed.edu)

SUPPLEMENTAL

1 Emissions sources
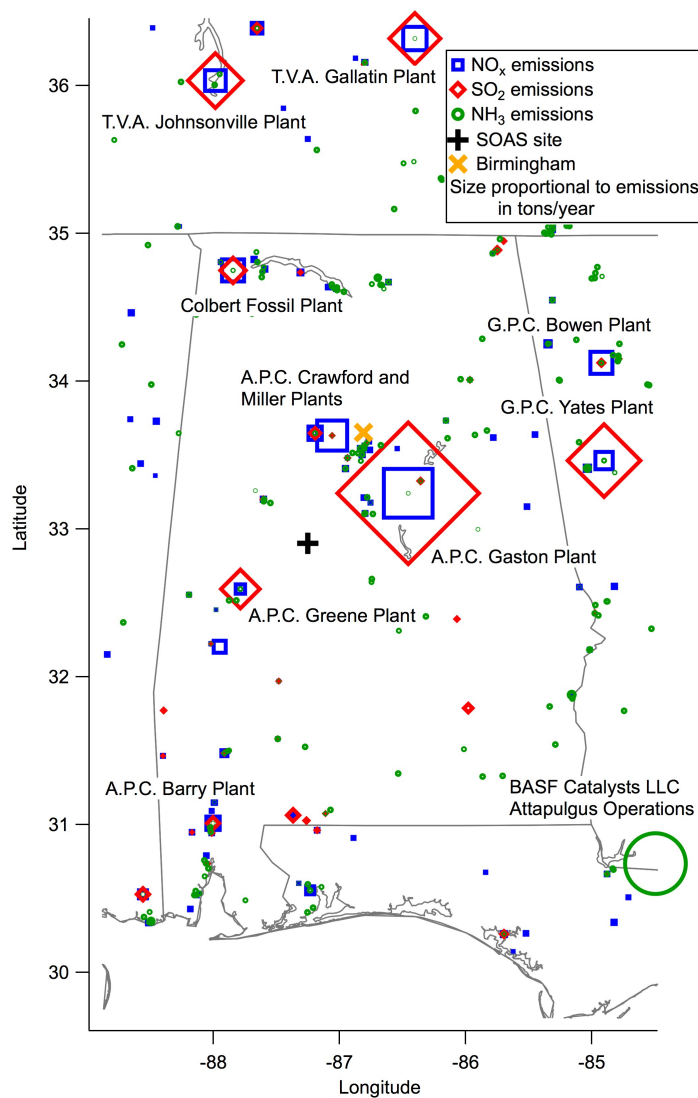
Figure S1: Point sources of SO$_2$, NO$_x$, and NH$_3$ in and around Alabama. Major pollution point sources include various electric generating plants primarily operated by the Alabama Power Company (APC), which emits 91,735 tons SO$_2$ per year and 16,982 tons NO$_x$ per year (Ernest C. Gaston plant), and the BASF Catalysists LLC - Attapulgus Operations, a mineral processing plant, that emits 1,946 tons NH$_3$ per year. The size of markers is proportional to emissions in tons per year, with NH$_3$ emissions multiplied by a factor of 10 relative to NO$_x$ and 20 relative to SO$_2$ for visual clarity.

The SOAS campaign site, located in central Alabama, is influenced by a number of anthropogenic emissions sources (see Figure S1). These sources include the city of Birmingham, AL located 71 km northeast of the site, and numerous coal-fired power plants owned by the Alabama Power Company (APC) located within a 50-mile radius of the sampling site. These power plants include the Ernest C. Gaston plant 45 miles northeast of the site, the William Crawford Gorgas and James H. Miller Jr. plants both 50 miles north of the site, and the Greene County plant 50 miles southwest of the site. Pollution sources and emissions obtained from the 2011 EPA National Emissions Inventory (http://www.epa.gov/ttnchie1/net/2011inventory.html).

Regional mobile on-road and off-road sources (not pictured) will also contribute significantly to NO_x concentrations at the site.

2 HNO_3 and NO_3^- measurements

The diurnal profile of temperature during the campaign is commensurate with the diurnal profile of predicted HNO_3 concentrations produced by the thermodynamic inorganic model ISORROPIA II (Figure 8 and S2). As indicated in Figure S2, the temperature increased in the morning just after 6:00 as the sun rose, peaked around 13:00-15:00 in the afternoon, and gradually decreased over the course of the evening and night to a low just before 5:00; the profile of ISORROPIA II followed the same pattern. The stronger diurnal cycle seen in ISORROPIA, which is higher in amplitude than the MARGA observed profile, suggests that the model might display a higher dependence on temperature for partitioning of nitrate to the gas phase than existed in the atmosphere at Centreville. However, the inlet line used in this study (1224 cm^3 total volume and 4.4 seconds residence time) may also have dampened the HNO_3 diurnal profile observed by the MARGA.
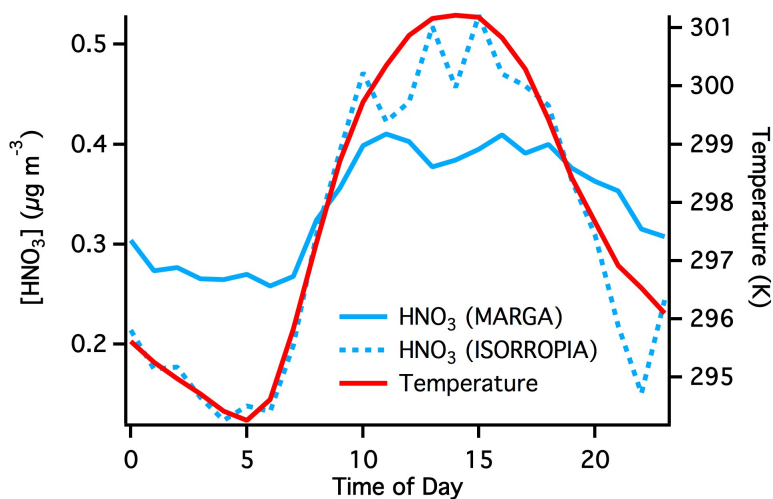
Figure S2: Diurnal profile of temperature (K) at the Centreville measurement site during the 2013 SOAS campaign compared with observed [HNO_3] (MARGA) and modeled partitioned [HNO_3] (ISORROPIA).

To check the robustness of the MARGA measurements of HNO_3 and NO_3^-, the MARGA measurements are compared to those available from two instruments collocated at the SOAS ground site at Centreville: a denuder-difference measurement made by Atmospheric Research and Analysis, Inc. (ARA) and a Chemical Ionization Mass Spectrometer (CIMS) made by the Wennberg group from the California Institute of Technology. The ARA instrument utilizes an inlet situated 5 m above ground level, with a flow rate of 1.25 L min^{-1}, residence time of less than 2 seconds, and sampling resolution of 1 minute. The instrument measures NO_3^- by difference in NO_y signal from a filtered versus unfiltered channel. Sample air in channel 1 (CH1) passes through a KCl-impregnated HEPA filter, then through a commercial molybdenum (Mo) mesh catalyst heated to 350 °C. The CH1 signal represents the measurement baseline for the analyzer, i.e., instrument dark current and any residual gas-phase NO_y not removed by the inlet lines and filter. Channel 2 (CH2) flows through a KCl-impregnated annular denuder (citric acid) into a parallel Mo converter also heated to 350 °C. The signal from CH2 includes baseline NO_y plus particulate nitrogen species that are convertible to NO. Because 350 °C Mo is essentially blind to reduced nitrogen (ammonia and particulate ammonium), this measurement assumes that nitrate is the only species of consequence (other than baseline NO_y) in the CH2 signal. HNO_3 is similarly measured by denuder difference (using 1% sodium carbonate solution as denuder wall coating), employing a Mo reduction converter and chemiluminescence (Edgerton et al., 2005).

2

The CIMS instrument is described in detail in Nguyen et al., 2014. Briefly, the instrument was located on the topmost platform of a metal walk-up sampling tower approximately 20 m in height (measurement heigh was approximately 22 m above ground). The CIMS employed a high-flow fluoropolymer-coated glass inlet (approximately 40 cm long, 3.1 cm ID) with a flow rate of 2,000 L min^{-1}. The analytical method utilizes a CF_3O^- reagent ion, calibrated for absolute sensitivity and water vapor dependence of ionization. The CIMS reports data as 5 second averages.

As indicated by a diurnal profile of HNO_3 measurements over the campaign timeframe, the three instruments measure slightly different concentrations of HNO_3 relative to each other. A substantially higher daytime HNO_3 peak exists in the ARA measurements compared to the MARGA measurement (Figure S3a). This discrepancy may be caused by a damping of the diurnal cycle of HNO_3 by MARGA from passivation of the TFE lines due to the relatively long residence time (4.4 s compared with less than 2 s for the ARA instrument) of the inlet line (Neuman et al., 1999). However, a third measurement by the CIMS, with a residence time of approximately 0.01 s, does not indicate a strong daytime HNO_3 peak but instead exhibits a diurnal profile more like that of the MARGA. This instrument was located at a substantially higher elevation than the MARGA inlet, and therefore might not be a direct comparison of HNO_3 concentrations, but indicates that dampening of the HNO_3 signal by the long MARGA inlet line does not fully explain the difference between the MARGA and ARA measurements. In addition, the ISORROPIA thermodynamic model (Figure S3c) predicts comparable magnitudes of NO_3^- and HNO_3 mass loadings to the MARGA during the day at the measured temperature and RH conditions of SOAS.
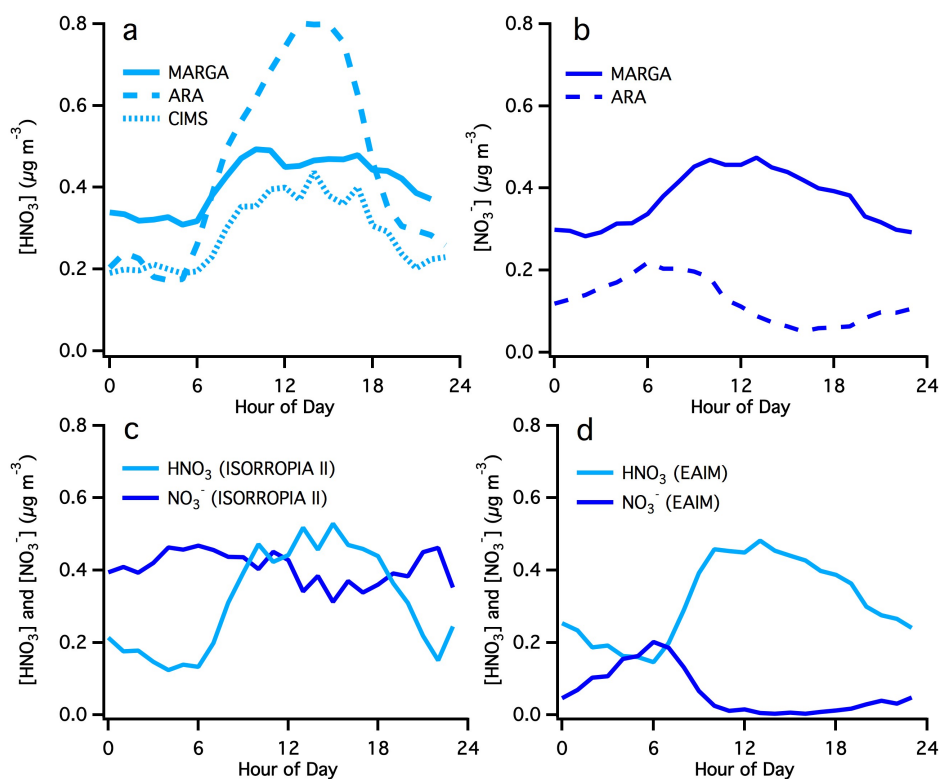
Figure S3: Diurnal profiles of gas phase HNO_3 averaged over 14 June and 3 July, and aerosol NO_3^- averaged over 1 June to 13 July, 2013 from 3 separate, collocated measurements and from modeling. (a) HNO_3 from MARGA, ARA, and CIMS measurements; (b) NO_3^- from MARGA and ARA measurements; (c) ISORROPIA II model predictions; and (f) EAIM (IV) model predictions. Refer to main body of paper for description of ISORROPIA and EAIM model runs.
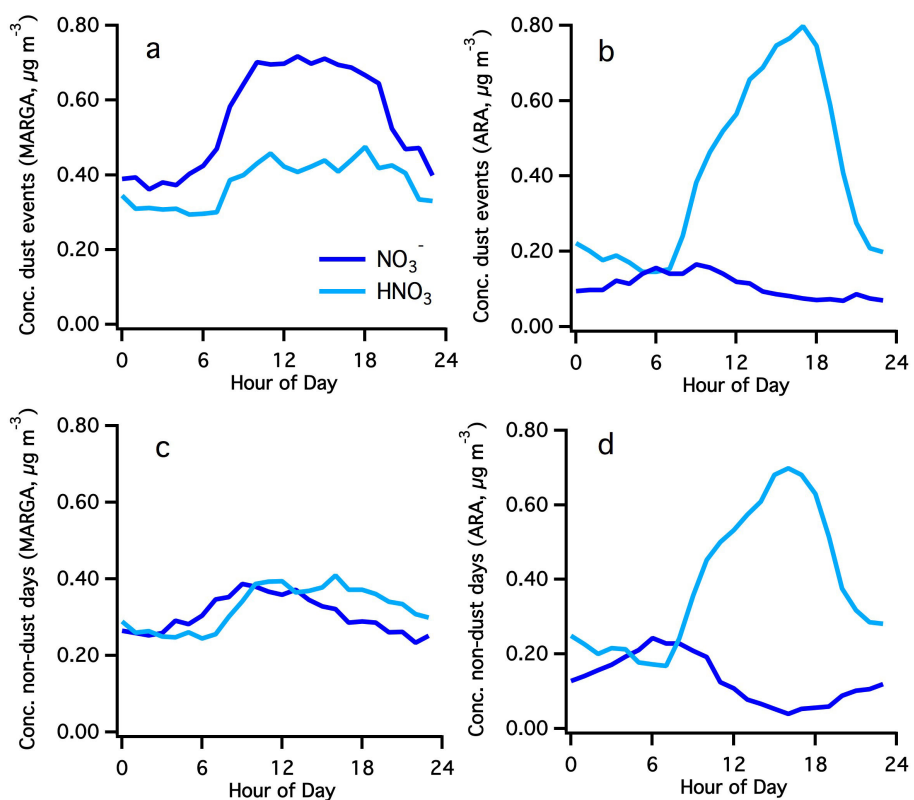
Figure S4: Comparison of HNO_3 and NO_3^- measurements during coarse particle events (panels a and b) and non-coarse particle events (panels c and d) periods measured by MARGA (left) and ARA (right) show evidence that the MARGA size cut may be larger than ARA and thus include more coarse mode NO_3^-. This analysis is consistent with the ambient size distribution during coarse particle events peaking near 3 μm in particle diameter (Figure S5), and with a laboratory test of the $PM_{2.5}$ cyclone used at SOAS showing that a non-negligible fraction of 3 to 5 μm diameter particles penetrate the cyclone at flow rates used in the field.
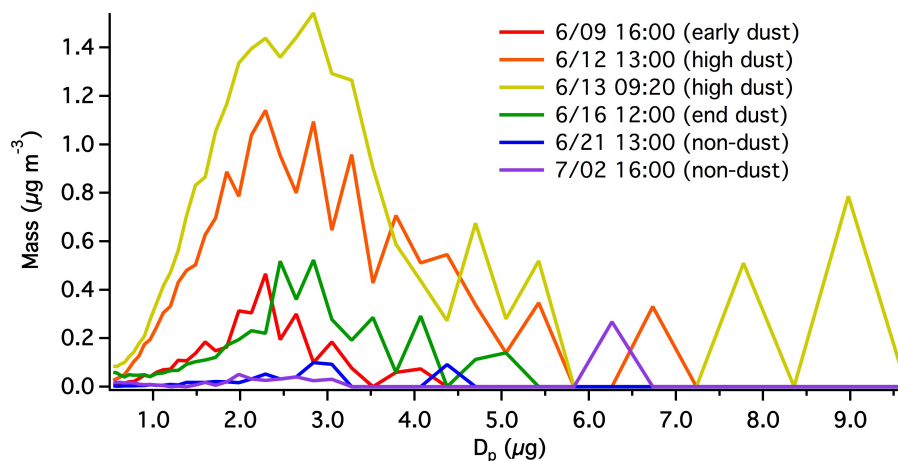
Figure S5: Mass distribution of aerosols of given diameters at times before, during, and after the second coarse particle event during the 2013 SOAS campaign. This distribution indicates peak mass loading occurred near 3 μm, indicating that small discrepancies in instrument inlet PM2.5 size cut could lead to large differences in measured NO_3^- concentrations.
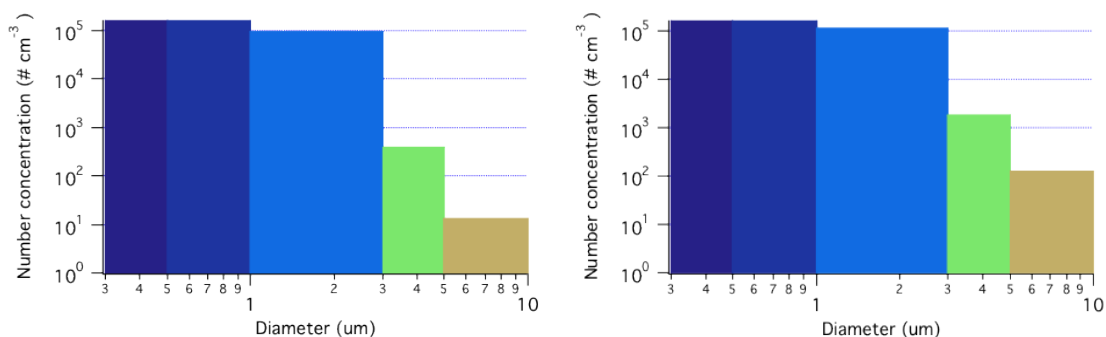
Figure S6: Number size distribution of Portland, OR particles (left) pulled through the PM$_{2.5}$ cyclone used with the MARGA inlet during the SOAS campaign at 16.7 lpm, and (right) without the cyclone, in both cases averaged for several interleaved 5 minute intervals during which particle size distribution was constant. Approximately 20% of particles in the 3 to 5 μm size range and 10% in the 5 to 10 μm size range transmit through the cyclone. During dust events at SOAS, the particle size distribution peaked near 3 μm, suggesting that slight differences in PM$_{2.5}$ size cuts of instrument inlets could have a substantial effect on measure aerosol concentrations.
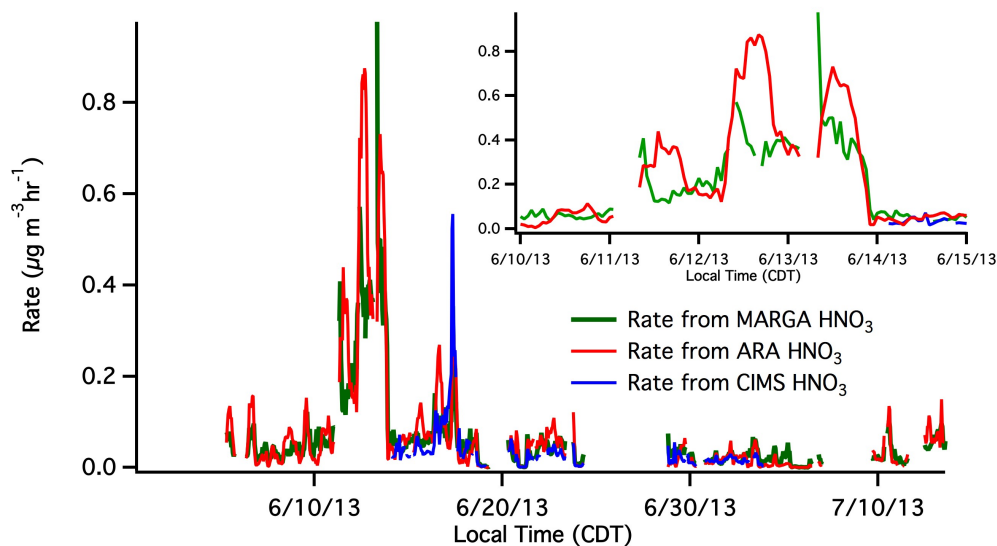
Figure S7: Comparison of the rate of HNO$_3$ uptake on mineral dust (see section 3.5) employing HNO$_3$ measurements made by MARGA, the ARA instrument, and by CIMS, with inset showing the predicted rate for the first coarse particle event. The discrepancies in measured HNO$_3$ do not appear to significantly alter the magnitude of the predicted uptake rate.

During the campaign, the MARGA measured higher aerosol NO$_3^-$ loading than similar measurements by the ARA instrument (Figure S3b). The diurnal profile of the MARGA measurements indicates a pronounced midday NO$_3^-$ peak; by contrast, ARA measurements indicate highest NO$_3^-$ concentrations in the early morning. In addition, a comparison of diurnal averages for NO$_3^-$ made by MARGA and the ARA instrument during coarse particle and non-coarse particle events indicates that the MARGA measures substantially higher NO$_3^-$ during the coarse-particle events (Figure S4). The discrepancy between the two NO$_3^-$ measurements may arise from the MARGA size cut being higher than the nominal PM$_{2.5}$ cutoff of the new URG cyclone installed for this campaign (see Methods section 2.2.1), which was designed to match the instrument inlet flow rate of 16.7 lpm. During the dust events, the peak in mass loading occurs near the 2.5 μm cut point of the cyclone (Figure S5), suggesting that even small differences in the cut point of the

ARA and MARGA inlets could lead to large differences in measured NO_3^- concentrations. Flows through the MARGA inlet were monitored continuously in the field, but subsequent testing of the $PM_{2.5}$ inlet suggests that approximately 20% of particles in the 3 to 5 μm size range and 10% of particles in the 5 to 10 μm size range transmit through the cyclone (Figure S6). Alternatively, the ARA measurement could be under-measuring concentrations of $PM_{2.5}$ nitrate, due to less than 100% Nylon collection and extraction efficiencies; however, these losses are minor (less than 10%). Both of these possibilities are consistent with the dust event uptake occurring predominately onto coarse-mode particles, which would be more efficiently detected by the MARGA rather than the ARA monitors. In addition, the E-AIM model output matches the ARA NO_3^- measurement more closely than that of the MARGA measurement (Figure S3d). Because E-AIM omits mineral cations, this result is consistent with the MARGA measuring dust-derived nitrate and the ARA system measuring predominately fine mode NH_4NO_3.

Although differences exist between the three HNO_3 measurements and the two NO_3^- measurements, these discrepancies do not appear to substantially affect the predicted rate of HNO_3 heterogeneous uptake on mineral dust (see section 3.5). The rate derived from HNO_3 measurements made by the ARA instrument and by the CIMS are very similar to that derived from the MARGA HNO_3 measurements (Figure S7). The rate of uptake is driven primarily by the availability of coarse particle surface area (section 3.5), and therefore discrepancies in measurements of HNO_3 do not greatly impact the average rate at which NO_3^- forms in the aerosol phase from this process.

3 Historical data

Data collected at the Centreville measurement site provides a historical context for analysis of nitrate and mineral dust interactions. Figure S8 gives a year-long look at concentrations of crustal minerals compared with aerosol NO_3^- and shows the direct correlation between the two. Table S1 shows values of acidity, defined as the slope of $[SO_4^{2-}]$ vs. $[NH_4^+]$ (in μEq m^{-3}) correlations for each year, along with the number of sea salt and mineral dust events that year. Sea salt events are defined as the number of points (3-day averages) of the ratio Cl^-/Na^+ at or above a value of 1.164. Mineral dust events are defined by the number of points (3-day averages) of nss-Na^++Ca^{2+} at or above a value of 0.1 μg m^{-3}. The sea salt and mineral dust events, and their correlation with NO_3^- occur throughout the year, but most frequently during the spring and summer months when temperatures are warmer than later in the year.
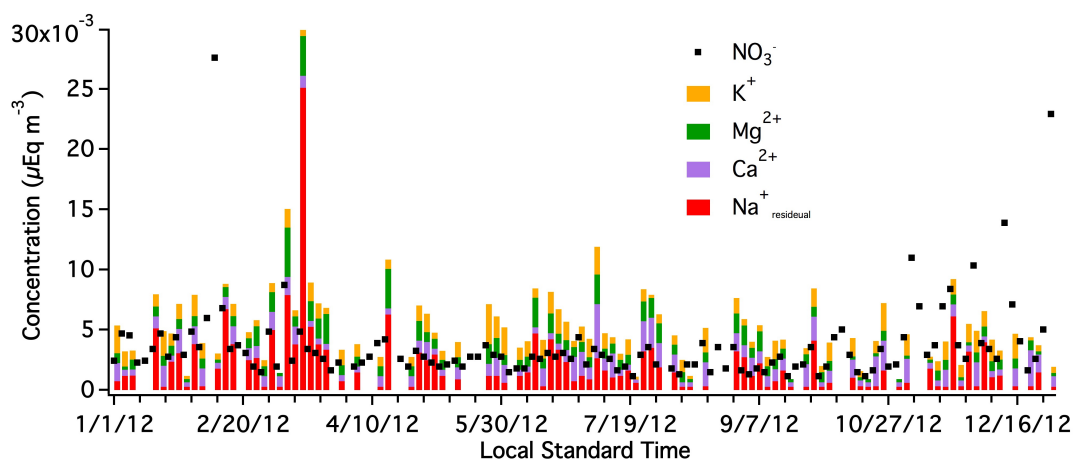
Figure S8: Time series showing concentrations of stacked K^+, Mg^{2+}, Ca^{2+}, and $Na^+_{residual}$ (Na^+ subtracting Cl^- equivalents) compared with NO_3^- for the year 2012 at the Centreville measurement site.

Table S1: Historical acidity, number of sea salt events, and number of mineral dust events for the Centreville measurement site from 2008-2012. The 2013 SOAS campaign had an acidity value of 1.12, similar to those of previous years.

Year	Acidity	Sea Salt Events	Mineral Events
2012	1.2	26	20
2011	1.08	20	24
2010	1.11	42	21
2009	1.16	37	12
2008*	1.12	28	14

Data collected using Teflon filters (ARA); *Note: 2008 begins April 19

References

Edgerton, E. S. and Hartsell, B. E. and Saylor, R. D. and Jansen, J. J. and Hansen, D. A. and Hidy, G. M. (2005). "The Southeastern Aerosol Research and Characterization Study: Par II. Filter-based measurements of fine and coarse particulate matter mass and composition." *J. Air and Waste Manage. Assoc.*, 55:1527-1542.

Neuman, J. A. and Huey, L. G. and Ryerson, T. B. and Fahey, D. W. (1999). "Study of inlet materials for sampling atmospheric nitric acid." *Environ. Sci. Technol.*, 33:1133–1136.

Nguyen, T. B. and Crounse, J. D. and Teng, A. P. and St. Clair, J. M. and Paulot, F. and Wolfe, G. M. and Wennberg, P. O. (2014). "Rapid deposition of oxidized biogenic compounds to a temperate forest." *PNAS*, 112:E392-E401.